TECHNICAL UNIVERSITY OF CLUJ-NAPOCA

ACTA TECHNICA NAPOCENSIS

Series: Applied Mathematics, Mechanics, and Engineering
Vol. 67, Issue I, March, 2024

NUMERICAL INVESTIGATION ON SHEAR RESISTANCE OF RC BEAMS WITH DOWEL ACTION UNDER GENERAL LOADING

Sreenivasa Prasad JOSHI, Poluraju PALLEBOINA

Abstract: *The study of shear strength of reinforced concrete beams was always a challenging for many researchers as lot of complexity involved in determining the contribution of each factor. In the recent experimental investigation conducted by the authors it was determined that 'V_a' and 'V_d' are negligible in shear resistance of concrete beams and 'V_{cz}' plays a major role in determining the shear resistance with shear reinforcement provided. The present article is aimed at validating the experimental results obtained with Finite Element Module 'ANSYS'. Regression analysis was carried out and corrected factor was applied to the previous empirical formula as proposed by the researchers and suitable empirical formula is formulated to evaluate the dowel force with shear reinforcement. To that aim, total sixteen specimens were cast and tested with increase in strength of concrete and variation in flexural reinforcement by keeping clear cover and effective span to depth ratio constant. For eight specimens preformed cracks were provided to eliminate aggregate interlocking effect and rest of eight specimens were controlled beams. Initially, the moment vs. displacement curvature and strain vs. moment curvature responses were studied with the experimental values obtained to appraise the shear at uncracked compression zone and later aggregate interlocking force and dowel action were obtained based on the empirical expressions proposed by previous researchers.*

Key words: *Aggregate interlocking, Dowel action, Finite Element Module, Regression analysis, Corrected factor.*

1. INTRODUCTION

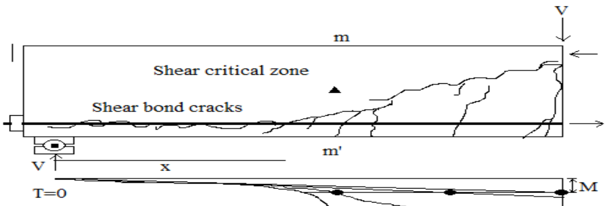

Fig. 1: Tensile stress distribution of longitudinal reinforcements at shear failure (Kim *et al.* 2018)

RC beams are exposed to shear and bending moment which primarily progress flexural cracks at the bottom mid and with increment in load, flexural cracks intensify which progress to m–m' position as represented in the Fig. 1. Under multiaxial stress, flexural cracks at the m–m' location do not occur in the extent of '*x*'. It is implicit that, the distance of diagonal cracks and flexural cracks from support and the shear resistance of RC beams are influenced by shear- span-to-depth ratio and longitudinal reinforcement ratio. The flexural occurring at the last progresses into flexural-shear cracks and the RC beams fails because of shear along the longitudinal reinforcements. As shown in figure 1, the extreme stress gradient, the stress distribution of longitudinal reinforcement at shear failure is non-linear from the supporting point which is observed up to m–m', representing bond stress which indicates maximum stress is displayed near the m–m' cross section. Beams without shear reinforcement were expected to have undergone shear bond failures which were produced due to rise in local bond stress at '*x*' and during the process diagonal cracks develop at m–m' followed by the quick spreading of shear bond failures over the range of '*x*' and finally failure (Fig. 2).

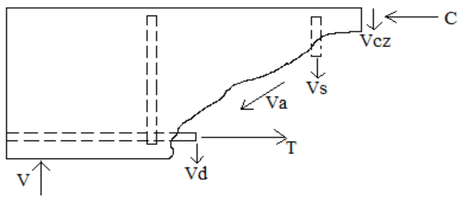

Fig. 2: Shear transfer mechanism in beam

Received: 30.09.23/29.01.24; **Similarities**: 07.03.24: **Reviewed**: 09.12.23/15.02.24: **Accepted**:23.03.24.

Shear is transferred among two adjacent planes in RC beam by the following mechanisms:

a) V_{cz} - Shear resistance of the uncracked portion of the concrete
b) V_{ay}- Critical component of the interface shear or aggregate interlock force V_a
c) V_d - Dowel force in the tension reinforcement due to dowel action.

Thus, $V= V_{cz} + V_{ay} + V_d$. (1)

The contribution of each component mentioned above rest on the stage of loading and extent of cracking. At the beginning, before flexural crack occurs, the entire shear is opposed by shear

$$V_{cz} = E_c \quad V \quad \frac{\delta\varepsilon}{\delta M}$$

resistance of the concrete (i.e., $V = V_{cz}$). As the flexural crack propagates, boundary of shear arises into action and relocation of stresses takes place, which advances and allow the crack to propagate resulting in distribution of shear by the dowel force V_d of the flexural reinforcement. At the failure, the shear is allowed by all the three mechanisms as represented in Eq. 1 and contribution of each component in shear transfer mechanism are in the range of 20 to 40% for V_{cz}, 30 to 50% for V_{ay} and 15 to 25% by V_d.

Sarkar *et al.* (1999) in his study had eliminated aggregate interlocking force as presented in Fig. 3.

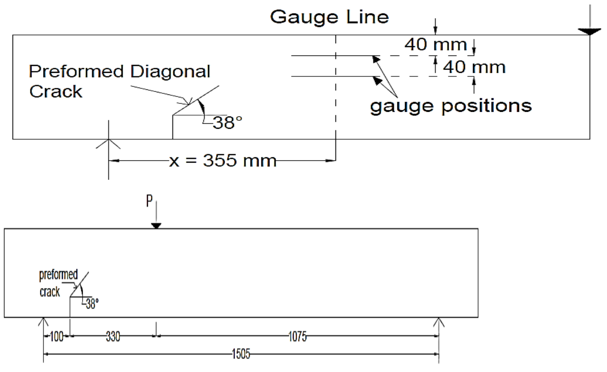

Fig. 3: Procedure by "Sarkar *et al.* (1999)"

They conducted beam end type testing on high strength RC beam. They divided the specimens into two categories. One group of samples were controlled beams and second group of samples were beams with preformed cracks (to eliminate aggregate interlocking force) where shear cracks were inclined at an angle of 38°.

The shear stress equation in uncracked concrete was determined from the equation as proposed by Taylor (1970).

$$V_{CZ} = \int_0^y \frac{\delta\sigma}{\delta M}\frac{\delta M}{\delta X}dY \quad (2)$$

Authors (2021) in their experimental work had modified the equation as proposed by Taylor(1970) and modified as represented in the Eqn. 3.

Then dowel force can be evaluated as $V_d = V- V_{cz}$. Zararis and Papadakis (2001concluded that, compression zone in concrete('V_{cz}') was the major contributor in shear resistance of beams and aggregate interlocking and dowel action have minimum contribution in resisting the diagonal tension cracks. Panda and Apparao (2017) had proposed experimental formula as represented in Eq.4 for determining the dowel force by applying predetermined cracks and maintaining the a/d ratio constant.

$$V_d = 0.311 + 0.221p\phi - 0.064pf_{cu} + 0.29C0 - 0.484p\phi C0 + 1.201p\phi f_{cu}C0 \quad (4)$$

Similarly, Kim *et al.* (2018), with varied percentages of shear span to effective depth ratio extending from 2.0-4.0, without shear reinforcement, had decided that role of 'V_a' was 18 – 30 % and 'V_d' was 25 – 30%. Empirical formula was projected by them to evaluate 'V_a' with shear reinforcement as represented in Eqs. 5 and 6.

$$V_a = 0.4\left(\frac{0.21f'c^{\frac{2}{3}}}{\gamma_c}\right)b.d(f'_c \leq 50MPa) \quad (5)$$

and

$$V_a = 0.4\left[1.48\,ln\left(1+\frac{f'c}{10}\right)\right]b.d(50MPa \leq f'_c \leq 90MPa) \quad (6)$$

From the above discussion, it was understood that there were great variations observed in different codes in defining the shear which is instigating to carryout research activity from past many years. Compression field models which were proposed earlier are being corrected by employing suitable variables. Aggregate interlock was overlooked and also lack of computational steps to evaluate shear at compression was found missing to evaluate dowel force. Secondly study of dowel force under flexural loading was found mislaid due to varying design variables and henceforth it was necessary to study the same by applying increase in strength of concrete and percentage of flexural reinforcement by keeping effective span to depth ratio and clear cover constant.

2. RESEARCH SIGNIFICANCE

The present study focused on structural behaviour of RC beams with shear reinforcement provided by employing suitable compressive strength of concrete and keeping a/d ratio constant.

- The theories or expressions applicable to evaluate factors in shear resistance for RC beams on which they are established display certain restrictions.
- Still substantial gap emerges in understanding the multifaceted behaviour of shear resistance of RC beams.
- Henceforth, there is a necessity to study shear resistance of RC beams integrating with different proportions of flexural reinforcement and by increasing the characteristic strength of concrete by preserving shear span to effective depth ratio and clear cover constant.

In present study, an effort has made to realize the contribution of each factor of shear resistance of RC beams for control beams and beams through elimination of aggregate interlocking force and to obtain suitable empirical formula to evaluate dowel force 'V_d'.

3. EXPERIMENTAL PROGRAMMING

The present investigation had focused mainly on various components in shear transfer mechanism and their contribution in shear resistance for varying proportions of flexural reinforcement for control beams and beams with preformed shear cracks. The study was focused on behaviour of failure of the beams and ultimate shear load carrying capacity. As rise in strength of concrete was also one of the parametric studies, M30 and M50 grade concrete was considered and total sixteen specimens of Fe500 steel were used.

Following Figs.4-6 represent detailing of RC beam with varying percentage of flexural reinforcement.

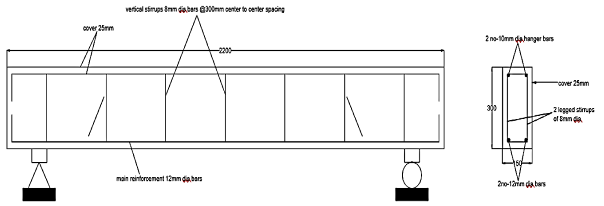

Fig.4: Cross Section of Beam with 0.6 Percentage of Flexural Reinforcement

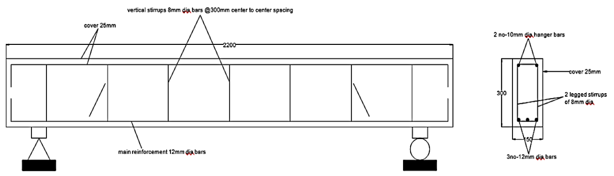

Fig. 5: Cross Section of Beam for 0.9 Percentage of Flexural Reinforcement

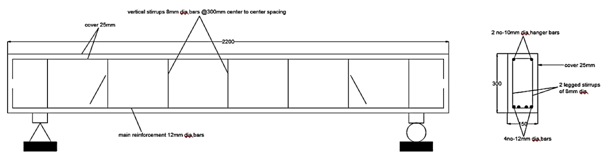

Fig. 6: Cross Section of Beam with 1.2 Percentage of Flexural Reinforcement

For casting of beams, initially design mix was carried out as per IS 10262:2009 and IS 456:2000.

For preformed cracks, an iron plate of size 260 mm × 170 mm × 5mm was taken. Marking of an angle of 45^0 was performed on the casting box at gap of 380mm equally at the ends and 60 mm from the bottom to a distance of 170 mm to fix. as represented in Fig. 7.

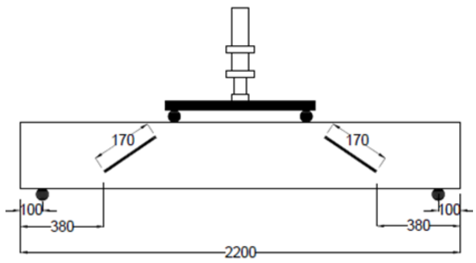

Fig. 7: Diagrammatic representation

Once the reinforcement was placed, concrete was poured and any air voids which were present were removed with the help of needle vibrator. Four hours after initial setting, plates were removed and specimens were kept twenty- eight days curing. Fig.8. denotes beam with preformed crack beam.

Fig. 8: Preformed crack beam

3.1 Testing Procedure

After curing, to know the ultimate load carrying capacity, beams were examined below four-point bending load. Two support conditions such as hinged support and roller support were placed to obtain static determinacy. Supports were positioned at 100 mm distance from both ends, where hinged and roller were positioned at the ends as represented in Fig. 9.

The loading frame was 200 tons capacity. To provide any irregularity it was necessary to afford plate and mortar. To obtain four-point loading, two-point was taken from I sectional girder which was positioned on the beam and the rest were arranged in the method of steel solid billets. To note down the readings, Linear Variable Deformation Transducer (LVDT) was sited at the mid lowest surface of the beam and loading cell was arranged to generate load *vs.* deflection response. Fig. 9., Represents diagrammatic representation of loading of the specimen and Fig.10., represents failure of the beam after testing.

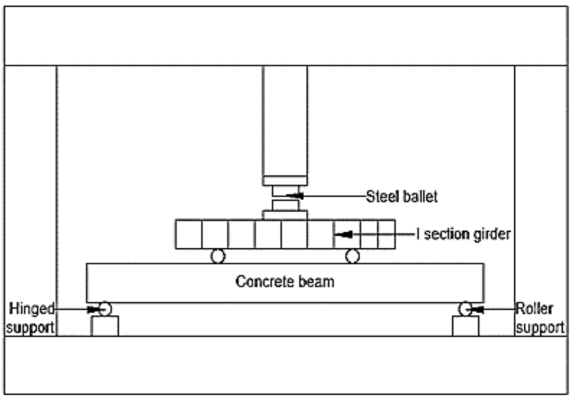

Fig. 9: Diagrammatic representation

Fig. 10: Preformed crack beam

The results obtained experimentally were compared with the suitable FEM module ‘ANSYS’ as discussed in Results and Discussions.

4.RESULTS&DISCUSSION

Following steps are involved

a. Assigning engineering data, which includes data of concrete and steel.
b. Modelling of reinforced concrete beam of span 2200 mm and cross section 150 mm×300 mm. Reinforcement to the beams has been varied for different percentages of flexural reinforcement (0.6%, 0.9% and 1.2%).
c. Modelling of I section girder.
d. Assigning loads
e. Run analysis and obtain results.

Following Figs. 11 and 12 represents modelling of control beam and preformed diagonal crack beams and Figs. 13 and 14 represents deflection of beams after assigning the loads where NA represents Numerical Analysis.

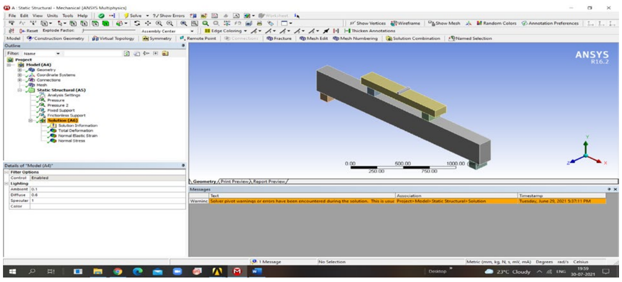

Fig. 11: Modelling of Control Beams

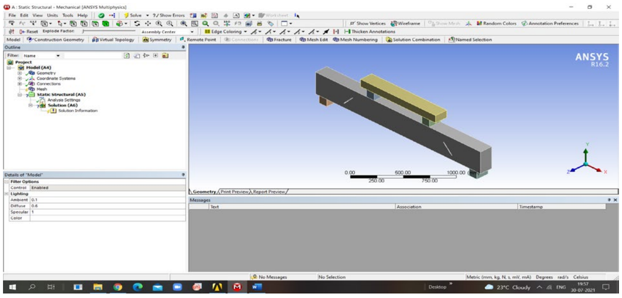

Fig. 12: Modelling of Preformed Shear Crack Beams

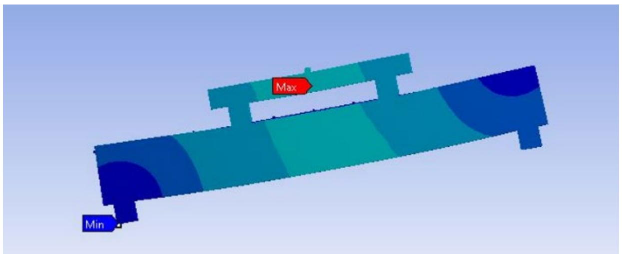

Fig. 13: Deflection of Control Beams

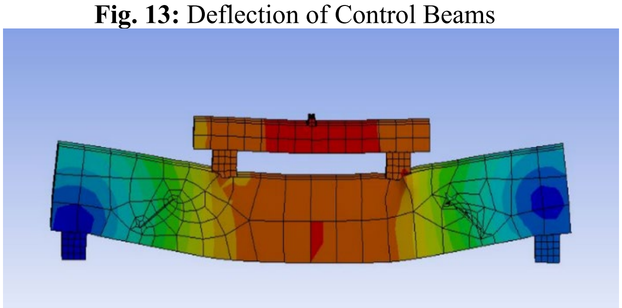

Fig. 14: Deflection of Preformed Shear Crack Beams

4.1. Results of M30 Grade Concrete Beams

The results obtained is presented in the section 4.1.1 and 4.2.2 in relationships of displacement *vs.* moment response and strain *vs.* moment response and ‘V’ and ‘V_{cz}’ are appraised.

4.1.1. Displacement *vs.* moment curve

Figs. 15 and 16, represents moment *vs.* displacement response and gradient at specific level stretches the value of ‘*V*’.

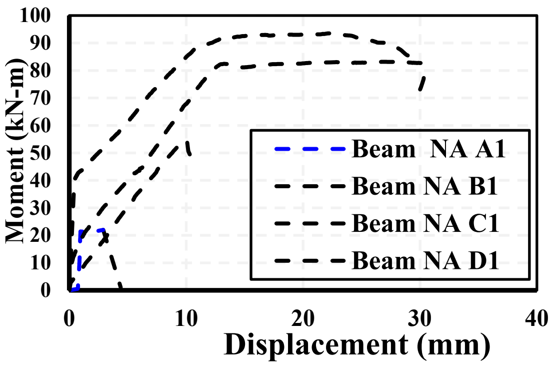

Fig. 15: Displacement *vs.* moment response for control beams (M30)

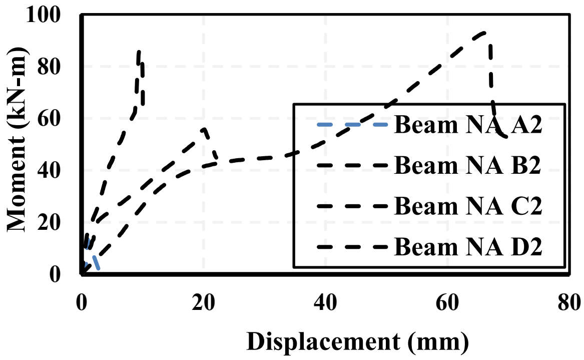

Fig. 16: Displacement *vs.* moment response for preformed diagonal cracks beams (M30)

From the above Fig.15, with the increase in load, the load-displacement curve of the specimen changed from linear elasticity failure in the initial stage to plastic properties. After reaching the peak load, the all specimens exhibited typical brittlefailure characteristics. The moment the axial force value becomes high it can be seen that the horizontal resistance force drops temporarily to a fairly low degree due to the combination of a decrease in plastic moment induced by axial force and the P-δ effect. Following are the failures for individual specimens, NAA1 at elastic limit, NAB1 at yield point, NAC1 and NAD1 strain hardening occurred before the failure and NAD1 a gradual drop was observed after failure, suggesting the ductility with the influence of lateral shear forces.

Fig. 16, with the elimination of aggregate interlocking force, decrease of shear cracks was observed with change in percentage of flexural reinforcement. A steady drop in the load was seen for entire specimens suggesting the ductility due to lateral shear forces. The specimen NA A2, failed immediately as there was no shear and flexural reinforcement provided. For remaining specimens NAB2, NAC2 failed after the yield point and NAD2 failed at ultimate load.

4.2.2 Strain *vs.* moment curve

Moment *vs.* strain response was appraised to determine shear at compression zone ‘V_{cz}’ as denoted in Eq.3 in introductory part, gradient at individual level evaluates ‘V_{cz}’ as signified in Figs. 17 and 18 respectively.

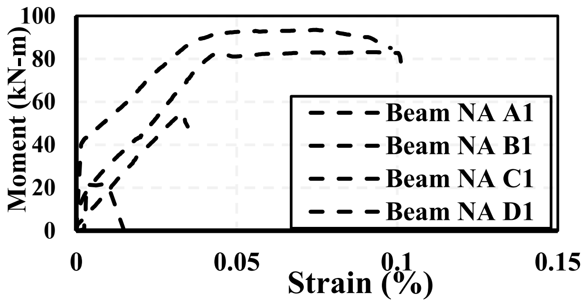

Fig. 17: Strain *vs.* moment response for control beams(M30)

From Fig. 17, after reaching the peak load a steady drip in the load was witnessed with increase in lateral strain. NAB1, NAC1, NAD1 ductile behaviour was observed due to lateral shear forces and also V_{cz} was increasing with varying flexural reinforcement.

From Fig. 18, after reaching the peak load a gradual drip in the load was witnessed with increase in lateral strain. NAB2, NAC2 and NAD2 ductile behaviour was observed under the lateral shear forces and also V_{cz} was increasing with rise in difference of flexural reinforcement.

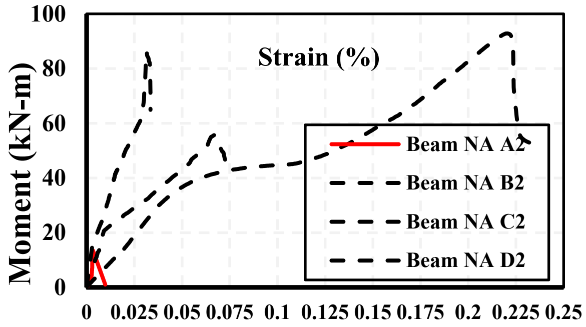

Fig. 18: Strain *vs.* moment response for preformed cracks (M30)

'V' and 'V_{cz}' are arrived based on the results obtained from Figs. 15 -18 and values attained are signified under Tables 1 and 2 respectively.

Table 1: 'V' and 'V_{cz}' for control beams

Beam designation	*V(kN)*	*V_{cz}(kN)*
NAA1	31.68	19.36
NAB1	44.57	26.75
NAC1	73.62	44.17
NAD1	81.09	48.65

Table 2: 'V' and 'V_{cz}' for preformed diagonal cracks

Beam designation	*V(kN)*	*V_{cz}(kN)*
NAA2	22.00	13.20
NAB2	47.23	28.33
NAC2	75.39	45.23
NAD2	81.48	48.89

From the Tables 1 and 2, it was discerned that contribution of 'V_{cz}' is more with the elimination of 'V_a' when compared with 'V_a' with varying flexural reinforcement.

4.2.3 Calculation of V_d

'V_d' are arrived based on the results obtained from Figs. 15 -18 and values attained are signified in Tables 3 and 4 respectively.

a) Control Beams

'V_a' was appraised built on the Eq.5 &6 as discussed in introductory part and the values attained are signified in Table 3.

Table 3: Controlled Beams

Beam Designation	*Reinforcement (%)*	*V_d(kN)*
NAA1	0	0
NAB1	0.6	25.25
NAC1	0.9	21.50
NAD1	1.2	16.60

b) Preformed cracks

Specimens with preformed cracks, V_a was eliminated and V_d was appraised based on Eq.1 as discussed in Chapter 1 and results attained are signified in Table 4

Table 4: Preformed cracks

Beam Designation	*Reinforcement (%)*	*V_d(kN)*
NAA2	0	0
NAB2	0.6	14.34
NAC2	0.9	10.91
NAD2	1.2	9.21

Values attained for 'V_d'is represented graphically as represented under Fig. 19, for control beams and with preformed crack.

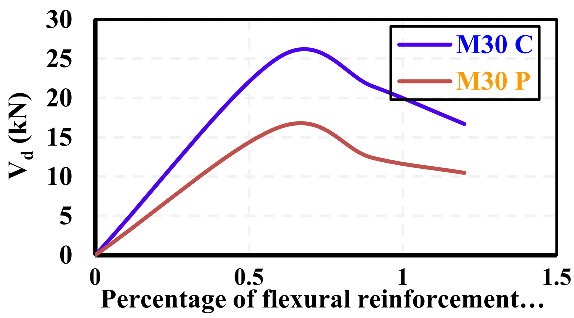

Fig. 19: 'V_d'(M30)

From the Fig. 19, influence of 'V_d' was reduced with the removal of 'V_a' and also declined with surge in percentage of flexural reinforcement for both control beams and preformed crack beams. Later, values arrived were compared with experimental formula as projected by Panda and Apparao (2017) Eq. 4 as presented in Table 5.

Table 5: Preformed cracks

Beam Designation	*Reinforcement (%)*	V_d*(kN)*	$V_{d(Appa\ Rao\ and\ Panda)}$ *(kN)*
NAA2	0	0	0
NAB2	0.6	16.31	23.93
NAC2	0.9	12.42	46.17
NAD2	1.2	10.48	69.22

From the above Table, it was apparent that, dowel force was increasing with varied flexural reinforcement which in accord as decided by researchers. There was noteworthy distinction among the theoretic and investigational values attained.

4.3. Results of M50 Grade Concrete Beams

Similarly, the results obtained is presented with respect to displacement *vs.* moment response and strain *vs.* moment response and 'V' and 'V_{cz}' are appraised in Figs.20 &21.

4.3.1. Displacement *vs.* moment curve

Figs. 20 and 21, represents moment *vs.* displacement response and gradient at specific level stretches the value of '*V*'.

From the Fig. 20, with the increase in load, the load-displacement curve of the specimen changed from linear elasticity failure in the initial stage to plastic properties. After reaching the peak load, the all specimens exhibited typical brittle failure characteristics.

The moment the axial force value becomes high it can be seen that the horizontal resistance force drops temporarily to a fairly low degree due to the combination of a decrease in plastic moment induced by axial force and the P-δ effect. Following are the failures for individual specimens, NAE1 at elastic limit, NAF1 at yield point, NAG1 and NAH1 strain hardening occurred before the failure and NAH1 a gradual drop was observed after failure, suggesting the ductility with the influence of lateral shear forces

Similarly, from the Fig. 21, with the elimination of aggregate interlocking force, reduction of shear cracks was observed with varying in percentage of flexural reinforcement. A gradual drop in the load was seen for entire specimens suggesting the ductility due to lateral shear forces. The specimen NAE2, failed immediately as there was no shear and flexural reinforcement provided. For remaining specimens NAF2, NAG2 failed after the yield point and NAH2 failed at ultimate load.

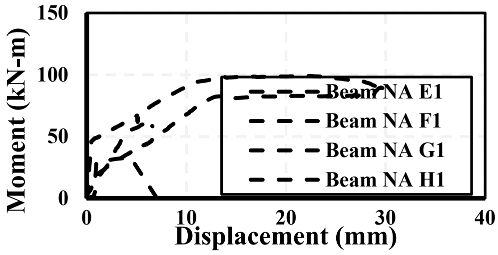

Fig. 20: Displacement *vs.* moment response for control beams (M50)

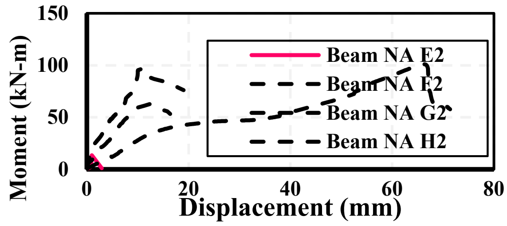

Fig. 21: Displacement vs. moment response for preformed crack (M50)

4.3.2. Strain *vs.* moment curve

Moment *vs.* strain response was appraised to determine shear at compression zone 'V_{cz}' as denoted in Eq.3 in introductory part, gradient at individual level evaluates 'V_{cz}' as signified in Figs. 22 and 23.

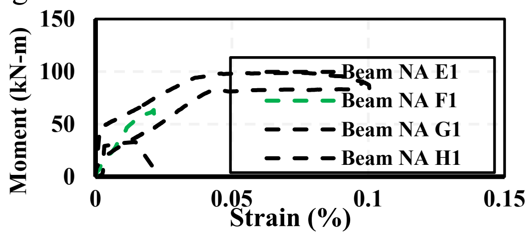

Fig. 22: Strain *vs.* moment response for controlled beams(M50)

From the above Fig. 22, after reaching the peak load a steady drip in the load was witnessed with increase in lateral strain. NAF1, NAG1, NAH1 ductile behaviour was observed due to lateral shear forces and also V_{cz} was increasing with varying flexural reinforcement.

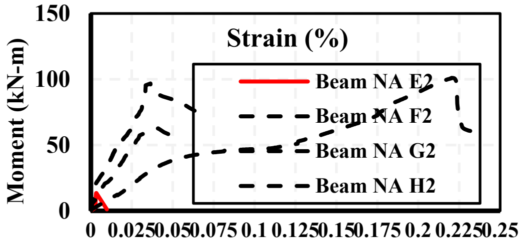

Fig. 23: Strain *vs.* moment response for preformed diagonal cracks beams(M50)

From the Fig. 23, after reaching the peak load a gradual drip in the load was witnessed with increase in lateral strain. NAF2, NAG2 and NAH2 ductile behaviour was observed under the lateral shear forces and also V_{cz} was increasing with rise in difference of flexural reinforcement. Results obtained from Figs. 20 - 23 were taken and *'V'* and *'V_{cz}'* are determined as discussed above and signified in Tables 6 and 7 respectively.

Table 6: '*V*' and 'V_{cz}' for control beams

Beam designation	*V(kN)*	*V_{cz}(kN)*
NAE1	32.08	19.36
NAF1	56.97	34.17
NAG1	81.00	48.60
NAH1	86.68	52.00

Table 7: '*V*' and 'V_{cz}' for preformed cracks

Beam designation	*V(kN)*	*V_{cz}(kN)*
NAE2	22.96	13.78
NAF2	53.12	31.87
NAG2	86.10	51.66
NAH2	89.62	53.77

From the Tables 6 and 7, it was discerned that contribution of 'V_{cz}' is more with the elimination of 'V_a' when compared with 'V_a' with varying percentage of flexural reinforcement

6.3.3 Calculation of V_d

'V_d' was assessed as proposed by Kim *et al.* (2018) in Eq. 6 as discussed in introductory.

a) Control Beams

'V_a' was appraised built on the Eq. 6 as discussed in introductory and the values of 'V_d' attained are signified in Table 8.

Table 8: Controlled Beams

Beam Designation	*Reinforcement (%)*	*V_d(kN)*
NAE1	0	0
NAF1	0.6	39.02
NAG1	0.9	31.68
NAH1	1.2	30.20

From the above table, 'V_d' was inclined to decline with surge in proportion of flexural reinforcement.

b) Preformed cracks

Specimens with preformed cracks, the shear donated by 'V_a' was removed and consequently shear contribution of 'V_d' was appraised. The subsequent are the outcomes attained, signified in Table 9, with rise in proportion of flexural reinforcement.

Table 9: Preformed cracks

Beam Designation	*Reinforcement (%)*	*V_d(kN)*
NAE2	0	0
NAF2	0.3	15.66
NAG2	0.6	12.83
NAH2	0.9	10.03

Values attained for V_d is represented graphically as represented in Fig. 24, for control beams and with preformed crack.

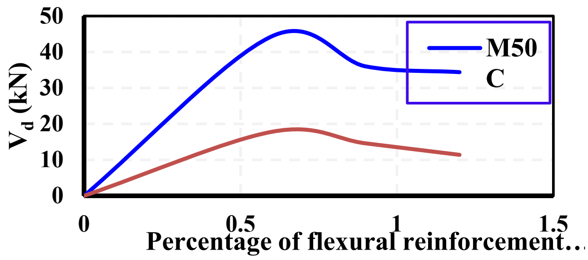

Fig. 24: 'V_d'(M50)

From the Fig. 24, contribution of 'V_d' was reduced with the removal of 'V_a' and also declined with surge in percentage of flexural reinforcement for both control beams and preformed crack beams.

Results obtained in 9 were compared with experimental formula as proposed by Panda and Apparao (2017) as mentioned in introductory part in Eq. 4 and represented in Table 10.

Table 10: Preformed cracks

Beam designation	*Reinforcement (%)*	*Experimental results(kN)*	$V_{d(Appa\ Rao\ and\ Panda)}$ (kN)
NAE2	0	0	0.30
NAF2	0.6	15.66	43.09
NAG2	0.9	12.83	87.87
NAH2	1.2	10.03	131.79

From the Table 10, eliminating V_a, value of V_d was inclined to surge with rise in proportion of flexural reinforcement which was in accord as determined. Noteworthy difference was seen between the theoretic and investigational values obtained.

6.4. Comparison of V_d of Numerical Values with the Experimental Values

The results obtained numerically were related with investigational values and the values attained are signified in Tables 11 – 13.

Table 11: Control beams

Beam	*Flexural Reinforcement (%)*	*Experimental Values (kN)*	*Numerical Values (kN)*
NAA1	0	0	0
NAB1	0.6	25.25	22.21
NAC1	0.9	21.50	18.92
NAD1	1.2	16.60	14.68

NAE1	0	0	0
NAF1	0.6	44.36	39.02
NAG1	0.9	36.09	31.68
NAH1	1.2	34.37	30.20

Table 12: Preformed crack

Beam	*Flexural Reinforcement (%)*	*Experimental Values (kN)*	*Numerical Values (kN)*
NAA2	0	0	0
NAB2	0.6	16.31	14.34
NAC2	0.9	12.42	10.91
NAD2	1.2	10.48	9.21
NAE2	0	0	0
NAF2	0.6	15.66	16.54
NAG2	0.9	12.83	13.71
NAH2	1.2	10.03	10.91

From the above tables it was clearly evident that values obtained numerically were similar to the experimental values obtained.

Values obtained numerically were also compared with the experimental formula as proposed by Panda and Apparao as presented in Table 13.

Table 13: Preformed cracks with empirical formula

Beam	*Flexural Reinforcement (%)*	*Experimental Values (kN)*	*Numerical Values (kN)*	$V_{d(Appa\ Rao\ and\ Panda)}$ **(kN)**
NAA2	0	0	0	0
NAB2	0.6	16.31	14.34	27.2
NAC2	0.9	12.42	10.91	52.47
NAD2	1.2	10.48	9.21	78.67
NAE2	0	0	0	0
NAF2	0.6	17.85	16.54	44.9
NAG2	0.9	14.65	13.71	88.88
NAH2	1.2	11.47	10.91	132.79

From the above table, vast variation was observed between the empirical values and numerical values.

Later Regression Analysis was conducted for both controlled beams and preformed cracks with Numerical values obtained and represented in Figs. 25-26.

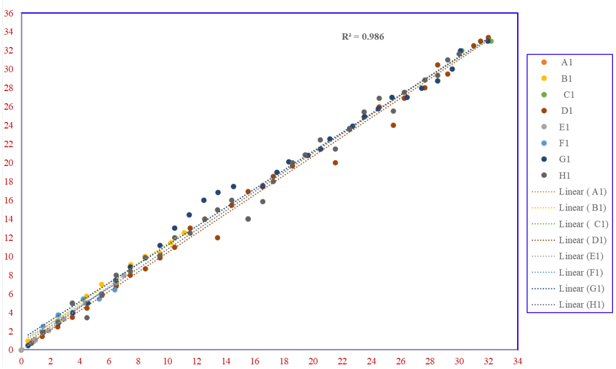

Fig. 25: Control beams

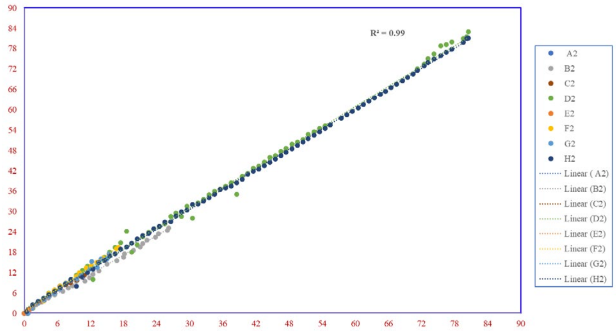

Fig. 26: Preformed crack beams

From the regression analysis it was clearly evident that there was not much variation between numerical values and experimental values obtained.

From the analysis, a corrected factor of 0.09 to be applied to Equation 4 and the new Equation proposed is represented in Equation 7 -$\boldsymbol{V_d = 0.311 + 0.221p\phi - 0.064pf_{cu} + 0.29C0 - 0.484p\phi C0 + 1.201p\phi f_{cu}C0}$ - 0.09 pf_{cu} (7)

The values obtained in Eqn. 7 is verified and represented in Table 14.

Table 14: 'V_d' Proposed formula

Beam	*Flexural Reinforcement (%)*	*Experimental Values (kN)*	*Numerical Values (kN)*	$V_{d(Proposed)}$ **(kN)**
NAA2	0	0	0	0
NAB2	0.6	16.31	14.34	16.20
NAC2	0.9	12.42	10.91	11.47
NAD2	1.2	10.48	9.21	8.67
NAE2	0	0	0	0
NAF2	0.6	17.85	16.54	15.90
NAG2	0.9	14.65	13.71	14.88
NAH2	1.2	11.47	10.91	10.79

5. CONCLUSION

Performance parameters, *viz.,* shear force V and shear at compression zone V_{cz} were evaluated from moment *vs.* displacement and moment *vs.* strain responses. Later aggregate interlocking force was calculated based on the pragmatic formula and contribution of elements in shear resistance of RC beams was identified from the results obtained experimentally. It was found that contribution of V_a and V_d were minimal and V_{cz} holds main involvement in shear resistance of RC beams. Experimental results obtained were also compared numerically with FEM module ANSYS and compared. Finally, results obtained were compared with empirical expression as suggested by Panda and Apparao

and new Equation was proposed as represented in Eqn.7.
The subsequent relevant conclusions are drawn from the present study.

1. With regards to control beams, contribution of V_{cz} was 38% - 40% and V_d was 15%-18%. Results obtained were similar to Zararis and Papadakis (2001) and Kim *et al.* (2018). Henceforth it was concluded that contribution of 'V_a' is minimum by keeping clear cover and $^a/_d$ ratio constant.
2. With elimination of 'V_a', similar results were obtained. Hence, effect of 'V_a' is negligible in shear transfer mechanism which were in agreement with Taylor (1970).
3. Similarly, contribution of 'V_d' was increased with varying proportion of flexural reinforcement and concrete strength which was agreed with Panda and Apparao (2017). Experimental formula proposed by them is not applicable as huge variations were observed with respect to experimental values obtained with shear reinforcement provided.
4. Analysis with Finite Element Modelling also obtained similar results with experimental results with a variance of 12%. Hence, it can be concluded that numerical analysis with Ansys is acceptable.
5. A new empirical expression $\boldsymbol{V_d = 0.311 + 0.221p\phi - 0.064pf_{cu} + 0.29C0 - 0.484p\phi C0 + 1.201p\phi f_{cu}C0}$ -0.09 pf_{cu} holds good to evaluate dowel force by eliminating aggregate interlocking with shear reinforcement provided.
6. Lastly, it was established that 'V_a' and 'V_d' are irrelevant in shear resistance of concrete beams and 'V_{cz}' is key contributor for shear resistance of diagonal tension cracks with shear reinforcement provided.

Nomenclature

a = Shear span (mm)
a/d = Shear-span-to-depth-ratio
b = Width of beam (mm)
C_0 = Cover (mm)
d = Depth of the beam (mm)
E_c = Modulus of elasticity of concrete (N/mm2)
f_{ck} = Compressive strength of concrete as per IS 456-2000 (N/mm^2)
f_{cu} = Grade of concrete
M= Moment at a distance X from support (N-mm)
P= Percentage of steel (%)
V= Shear force at support (N)
V_a = Aggregate interlocking force (N)
V_{cz} = Shear stress at a depth Y from the compressive face (N)
V_d = Dowel force (N)
W/C = Water cement ratio
δm= Moment at the given load and displacement
δε = Corresponding strain for the given displacement
δx = Corresponding displacement
ε = Strain
σ = Longitudinal stress at a distance 'x' from the support
φ = bar diameter (mm)
NAA1= Beam without shear and flexural reinforcement
NAB1= Beam with 0.3% flexural reinforcement
NAC1= Beam with0.6% flexural reinforcement
NAD1= Beam with 0.9% flexural reinforcement
NAE1= Beam without shear and flexural reinforcement
NAF1= Beam with 0.3% flexural reinforcement
NAG1= Beam with 0.6% flexural reinforcement
NAH1= Beam with 0.9% flexural reinforcement
NAA2= Beam without shear and flexural reinforcement
NAB2= Beam with 0.3% flexural reinforcement
NAC2= Beam with 0.6% flexural reinforcement
NAD2= Beam with 0.9% flexural reinforcement
NAE2= Beam without shear and flexural reinforcement
NAF2= Beam with 0.3% flexural reinforcement
NAG2= Beam with 0.6% flexural reinforcement
NAH2= Beam with 0.9% flexural reinforcement

6.REFERENCES

1. ACI Committee 318 (2019) "Building Code Requirements for Structural concrete and Commentary: Farming-ton Hills", MI: *American Concrete Institute*.
2. Angelakos, D., Bentz, E.C. and Collins, M.P. (2001) "Effect of concrete strength and minimum stirrups on shear strength of large members", *ACI Structural Journal*, 98(3), pp. 290-300.
3. Bazant, Z.P. and Gambarova, P.G. (1980). "Rough crack models in reinforced concrete", *ASCE-Journal of Structural Engineering*, 106(4), pp. 819-842.
4. Broo, H., Plos, M., Lundgren, K., Engström B. (2007) "Simulation of shear-type cracking and failure with non-linear finite-element method", *Magazine of Concrete Research*, 59(9), pp. 673-687.
5. Chana P.S. (1987) "Investigation of the mechanism of shear failure of reinforced concrete beams", *Magazine of Concrete*

Research, 39(141), pp. 196-204.

6. Dulacska, H. (1972) "Dowel action of reinforcement crossing cracks in concrete", *ACI Journal*, 69(12).
7. Eleiott, A.F. (1974) "An experimental investigation of shear transfer across crack in reinforced concrete", M.S. Thesis, Cornell University: Ithaca.
8. Feenstra, P.H., De Borst, R. and Rots, J.G. (1991) "Numerical Study on Crack Dilatancy I: Models and Stability Analysis", *Journal of Engineering Mechanics*, 117(4), pp. 733-753.
9. Fenwick, R.C. and Paulay, T. (1968) "Mechanisms of shear resistance of concrete beams", *Journal of the Structural Division (ASCE)*, 94(ST10), pp. 2235-2350.
10. Gergeley, P. (1969) "Splitting of Cracks along Main reinforcement in Concrete Members", *Dept. of Structural Engineering Report*, Cornell University.
11. Hamadi, Y.D. and Regan, P.E. (1980) "Behaviour of normal and lightweight aggregate beams with shear cracks", *The Structural Engineer*, 58B(4), pp. 71-79.
12. Houde, J. (1973), "Study of Force - Displacement Relationships for the Finite element Analysis of Reinforced Concrete", Structural Concrete Series No. 73-2, Mc Gill University,Montreal.
13. IS: 10262 (2009) "Concrete Mix Proportioning - Guide Lines". (Second Revision).
14. IS: 456 2000. Indian Standard Plain and Reinforced Concrete-Code of Practice (Fourth Revision).
15. Jelic, I., Pavlovic, M.N. and Kotsovos, M.D. (1999) "A study of dowel action in reinforced concrete beams", *Magazine of Concrete Research*, 51(2):131-14.
16. Kim, H.G., Jeong, C.Y., Kim, M. J., Lee, Y. J., Park, J.H., Kim, K.H. (2018) "Prediction of shear strength of reinforced concrete beams without shear reinforcement considering bond action of longitudinal reinforcements", *Advances in Structural Engineering*, 21(1), pp. 30-45.
17. Krefeld, W.J, Thurston, C.W, (1966). "Contribution of Longitudinal steel to Shear Resistance of Reinforced Concrete Beams", *ACI Journal*, 63(14), pp.67-74
18. Li, N., Maekawa, L., and Okamura, H. (1989) "Contact density model for stress transfer across cracks in concrete", *Journal of the Faculty of Engineering*, University of Tokyo, XL, pp. 9-52.
19. Li Y.-J. and Zimmerman T. (1998) "Numerical evaluation of the rotating crack model", *Computers and Structures*, 68, pp. 487-497.
20. Mathey, R.G. and Watsein, D. (1963) "Shear Strength of Beams without web Reinforcement Containing Deformed Bars of Different Yield Strengths". ACI Journal, 60(2), pp. 183-207.
21. Motamed, J. (1997). "Shear in normal strength and high strength reinforced concrete beamswith stirrups and horizontal web bars", MSc Thesis, *University of Westminster*, London.
22. Oh J.K. and Shin S.W. (2001) "Shear Strength of Reinforced High-Strength Concrete Deep Beams", *ACI Structural Journal*, 98(2), pp. 164-173.
23. Panda, SS and Apparao G (2017) "Study of dowel action in reinforced concrete beam by factorial design of experiment". *ACI Structural Journal*, 114(6), pp.1495-1505,
24. Pang, X. and Hsu, T.C. (1995) "Behavior of reinforced concrete membranes in shear", *ACI Structural Journal*, 92(6), pp. 665-679.
25. Paulay, T. and Loeber, P.J. (1974) "Shear transfer by aggregate interlock", *ACI - Special Publication*, SP42, pp. 1-15.
26. Qing Quang Liang, Yi Min Xie, and Steven G.P. (2000) "Topology Optimization of Strutand-Tie Models in Reinforced Concrete Structures Using an Evolutionary Procedure", ACI Structural Journal, 97(2), pp. 322-330.
27. Ramirez J.A, Olek J., and Malone B.J. (2004) "Shear Strength of Lightweight Reinforced Concrete Beams0', *ACI - Special Publication*, SP218-5.
28. Regan, P.E. (1993) "Research on shear: A benefit to humanity or a waste of time?", *The Structural Engineer*, 71(19), pp. 337-347.
29. Rots J.G. (2002) "Comparative study of crack models", *Finite Elements in Civil Engineering Applications*, pp. 17-29.
30. Rots, J.G. and De Borst, R. (1987) "Analysis of mixed-mode fracture in concrete", *Journal of Engineering Mechanics*, 113(11), pp. 1739-1758.
31. Sarkar, S. and Adwan, O. and Bose, B. (1999) "Shear Stress Contributions and Failure Mechanisms of High Strength Reinforced Concrete Beams", *Materials and Structures*, 32, pp. 112-116.
32. Singh, B. and Chintakundi, (2012) "An appraisal of dowel action in reinforced concretebeams" *In: Proceedings of Structures and Buildings*, 166(SB5).
33. Soltani M., An X., and Maekawa K. (2003) "Computational model for post cracking analysis of RC membrane elements based on

local stress-strain characteristics", *Engineering Structures*, 25, pp. 993-1007.

34. S.P. Joshi, P.Poluraju and Umesh K. Singh (2021) "Evaluation of Dowel Reinforcement with Shear Reinforcement Provided under Four Point Bending Load", *KSCE Journal of Civil Engineering*, 25(6), pp. 2143-2150.
35. Tan K.H. and Lu H.Y. (1999) "Shear Behavior of Large Reinforced Concrete Deep Beams and Code Comparisons", *ACI Structural Journal*, 96(5), pp. 836-845.
36. Taylor, H.P.J. (1970) "Investigation of the forces carried across cracks in reinforced concrete beams in shear by interlock of aggregate", *Technical report*, 42.447, CCA, London.
37. Vecchio, F.J. (1989) "Nonlinear Finite Element Analysis of Reinforced Concrete Membranes", *ACI Structural Journal*, 86, pp. 26-35.
38. Vintzeleou, E.N. and Tassios, T.P. (1987) "Behaviour of dowels under cyclic deformations". *ACI Structural Journal*, 84(1), pp. 18-30.
39. Vollum, R.L. and Newman, J.B. (1999) "Strut and tie models for analysis/design of external beam-column joints", *Magazine of Concrete Research*, 51(6), pp. 415-425.
40. Walraven, J.C. and Reinhardt, H.W. (1981) "Theory and experiments on the mechanical behaviour of cracks in plain and reinforced concrete subjected to shear loading", *Delft University of Technology*.
41. Watanabe, F. and Lee, J.Y. (1998) "Theoretical prediction of shear strength and failure mode of reinforced concrete beams", *ACI Structural Journal*, 95(6), pp. 749- 757.
42. Yang, K.H., Chung, H.S., Lee, E.T., Eun, H.C. (2003) "Shear characteristics of high strength concrete deep beams without shear reinforcement", *Engineering Structures*, 25(10), pp. 1343-1352.
43. Zararis, P.D. and Papadakis, G.Ch. (2001) "Diagonal shear failure and size effect in RC beams without web reinforcement", *Journal of Structural Engineering*, 127(7), pp. 733–742.
44. Zhang, N. and Tan, K.H. (2007) "Size effect in RC deep beams: Experimental investigation and STM verification", *Engineering Structures*, 29, pp. 3241-3254.
45. Zhang, L. and Hsu T.C. (1998) "Behavior and analysis of 100MPa concrete membrane elements", *Journal of Structural Engineering*, 124(1), pp. 24-34.

INVESTIGAREA NUMERICĂ A REZISTENȚEI LA FORFECARE A GRINZILOR RC CU ACȚIUNE DIBLU SUB SARCINĂ GENERALĂ

Rezumat: *Studiul rezistenței la forfecare a grinzilor din beton armat a fost întotdeauna o provocare pentru mulți cercetători, deoarece complexitatea implicată în determinarea contribuției fiecărui factor. În investigația experimentală recentă efectuată de autori s-a stabilit că "Va" și "Vd" sunt neglijabile în rezistența la forfecare a grinzilor de beton și "Vcz" joacă un rol major în determinarea rezistenței la forfecare cu armătură de forfecare furnizată. Prezentul articol are ca scop validarea rezultatelor experimentale obținute cu modulul cu elemente finite "ANSYS". Analiza de regresie a fost efectuată și factorul corectat a fost aplicat formulei empirice anterioare, așa cum au propus cercetătorii, și formula empirică adecvată este formulată pentru a evalua forța diblului cu armătură de forfecare. În acest scop, au fost turnate și testate în total șaisprezece specimene cu creșterea rezistenței betonului și variația armăturii la încovoiere prin menținerea constantă a acoperirii clare și a raportului efectiv anvergură-adâncime. Pentru opt exemplare au fost prevăzute fisuri preformate pentru a elimina efectul de centralizare a agregatelor, iar restul de opt exemplare au fost grinzi controlate. Inițial, răspunsurile la curbura moment vs. deplasare și deformare vs. curbură moment au fost studiate cu valorile experimentale obținute pentru a evalua forfecarea la zona de compresie nefisurată și ulterior forța agregată de interblocare și acțiunea diblului au fost obținute pe baza expresiilor empirice propuse de cercetătorii anteriori.*

Cuvinte cheie: *centralizare agregată, acțiune diblu, modul cu element finit, analiză de regresie, factor corectat*.

Sreenivasa Prasad JOSHI, *1 M.Tech, Ph.D. Assistant Professor, Department of Civil Engineering, Anurag University, Hyderabad, Telangana, India- 500088. Email: joshice@anurag.edu.in, joshiphd2378@gmail.com. Contact:+916281451711*

Poluraju PALLEBOINA *M.Tech, Ph.D. (IITM), Professor, Department of Civil Engineering KL(Deemed to be University), Vaddeswaram, Vijayawada, Andhra Pradesh, India-522502. Email: rajupolup@kluniversity.in, rajupolup@gmail.com.Contact: +919966018814*